

## Short communication

## Lanthanide complexes of anthraquinone-1,8-disulfonate: Syntheses, structures and catalytic studies

Fu-Yu Cao<sup>a</sup>, Meng-Ping Huang<sup>a</sup>, Hui-Lei Gao<sup>b</sup>, Xiao-Li Zhao<sup>c,\*</sup>, Jie Han<sup>d,\*</sup>, Xu-Dong Chen<sup>a,e,\*</sup><sup>a</sup> Jiangsu Collaborative Innovation Center of Biomedical Functional Materials and Jiangsu Key Laboratory of New Power Batteries, School of Chemistry and Materials Science, Nanjing Normal University, Nanjing 210023, Jiangsu, China<sup>b</sup> Chemistry Group, Dongying Chenyang School, Dongying District, Dongying City 257000, Shandong Province, China<sup>c</sup> Shanghai Key Laboratory of Green Chemistry and Chemical Processes, Department of Chemistry, East China Normal University, Shanghai 200062, China<sup>d</sup> School of Science & Technology, The Open University of Hong Kong, Kowloon, Hong Kong Special Administrative Region, China<sup>e</sup> State Key Laboratory of Coordination Chemistry, Nanjing University, Nanjing 210093, Jiangsu, China

## ARTICLE INFO

## Keywords:

Anthraquinone-1,8-disulfonate  
Lanthanide coordination compounds  
Catalysts  
Oxidation  
Sulfoxide

## ABSTRACT

Two isostructural series of four lanthanide coordination complexes have been synthesized by hydrothermal method with anthraquinone-1,8-disulfonate as the anionic ligand. The complexes also comprise  $K^+$  ions that participate into coordination to form bimetallic complexes. The ligands in these complexes chelate to either lanthanide or  $K^+$  ions, and in some circumstance bridge the ions as well. Besides inter-/intra-molecular hydrogen bonding between the sulfonate groups and water molecules,  $\pi$ - $\pi$  stacking interactions also contribute to the stabilization of the crystal packing. Investigation of the catalytic properties of the complexes indicated that they were able to promote the oxidation reaction of thioethers into sulfoxides, in which the  $Er^{3+}$  coordination complex exhibited the best catalytic efficiency over a wide range of substrates.

## 1. Introduction

Lanthanide coordination polymers (Ln-CPs) constructed by lanthanide ions and organic ligands [1] have attracted a lot of research interest because of their great promise for the development of materials with potential applications in areas such as gas adsorption and separation [2–5], tunable luminescence [6–11], proton conductivity [3,12], chemical sensing [13–18], and catalysis [19–25]. These unique properties mainly arise from 4f electrons of the lanthanide ions or the organic ligands, as well as the interactions between them that produce synergistic effect [1,7,14]. Lanthanide ions have high and variable coordination numbers with flexible coordination geometry adaptive to versatile frameworks [1].

Since lanthanide ions have a strong coordination affinity for oxygen [26], we utilized a sulfonate functionalized anthraquinone ligand for the construction of novel lanthanide coordination polymers. Compared to the widely used coordination group of carboxylate, sulfonate group are less employed as the coordination group in organic ligands [27–31].

This is because sulfonate group is “soft” in terms of coordination characters and is less favorable by transition metal ions in forming coordination complexes [32]. However, the sulfonate group coordinates with lanthanide ions very well and its steric feature allows more structural diversity [26,29]. On the other hand, the anthraquinone was selected for modification because of the rich redox properties of quinone compounds [33,34]. The redox processes of quinone compounds are commonly accompanied by single electron transfer or proton coupled electron transfer [35,36], dictating their potential applications in catalysis [37–39]. This property might be transferable into their coordination complexes and the catalytic efficiency might even be strengthened in certain cases due to synergistic effect. Therefore, the lanthanide coordination complexes of anthraquinone-1,8-disulfonate were synthesized and characterized, and their catalytic properties were studied.

The oxidizing reaction of sulfides into sulfoxides was selected as the substrate reaction. Sulfoxides are important industrial intermediates [40], but the over oxidation of thioethers may result in the generation of sulfones instead of sulfoxides [41,42]. Therefore, the controlled

\* Corresponding authors at: Shanghai Key Laboratory of Green Chemistry and Chemical Processes, Department of Chemistry, East China Normal University, Shanghai 200062, China (X.-L. Zhao); School of Science & Technology, The Open University of Hong Kong, Kowloon, Hong Kong Special Administrative Region, China (J. Han); Jiangsu Collaborative Innovation Center of Biomedical Functional Materials and Jiangsu Key Laboratory of New Power Batteries, School of Chemistry and Materials Science, Nanjing Normal University, Nanjing 210023, Jiangsu, China (X.-D. Chen).

E-mail addresses: [xlzhao@chem.ecnu.edu.cn](mailto:xlzhao@chem.ecnu.edu.cn) (X.-L. Zhao), [chan@ouhk.edu.hk](mailto:chan@ouhk.edu.hk) (J. Han), [xdchen@njnu.edu.cn](mailto:xdchen@njnu.edu.cn) (X.-D. Chen).

<https://doi.org/10.1016/j.inoche.2021.108682>

Received 19 March 2021; Received in revised form 29 April 2021; Accepted 17 May 2021

Available online 20 May 2021

1387-7003/© 2021 Elsevier B.V. All rights reserved.

oxidation of thioethers into sulfoxides has received extensive attention in recent years [42,43]. Despite extensive research on the selective oxidation of thioethers into sulfoxides, it is still of great importance to develop efficient catalyst with good product selectivity.

## 2. Experimental section

### 2.1. General

All reagents and solvents were purchased from commercial sources and used without further purification. Thermal analyses were carried out on a Mettler-Toledo TGA/DSC STARE system in the temperature range of 28–800 °C with a heating rate of 10 °C·min<sup>-1</sup>, under nitrogen flow. Infrared spectra were recorded on a VECTOR 22 spectrometer with pressed KBr pellets in the range of 4000–400 cm<sup>-1</sup>. Powder X-ray diffraction (PXRD) was done with a MiniFlex 600 X-ray powder diffractometer equipped with a Cu sealed tube ( $\lambda = 1.54178 \text{ \AA}$ ) at 40 KV and 40 mA. <sup>1</sup>H and <sup>13</sup>C NMR spectra were obtained in CDCl<sub>3</sub> solvent on a Bruker 400 MHz spectrometer. Elemental analyses were performed using a PE-240C elemental analyzer.

{[LnK(AQDS)<sub>2</sub>(H<sub>2</sub>O)<sub>4</sub>]·3H<sub>2</sub>O}<sub>n</sub> (Ln = La (1) and Nd (2)). These compounds were prepared by the same procedure as follows. A mixture of lanthanide salt (La(NO<sub>3</sub>)<sub>3</sub>·6H<sub>2</sub>O (14.3 mg, 0.033 mmol) or NdCl<sub>3</sub>·6H<sub>2</sub>O (11.8 mg, 0.033 mmol)) and K<sub>2</sub>AQDS (dipotassium anthraquinone-1,8-disulfonate, 22.2 mg, 0.05 mmol) in 2 mL H<sub>2</sub>O was placed in a 10 mL glass vial. After ultrasonic treatment for 20 min, the sample was heated at 100 °C for 12 h, and then cooled to room temperature. The resulting pale yellow needle-like crystals were collected by filtration, washed with methanol, and dried under vacuum. Yield: 78% for 1; 80% for 2. Elemental analysis for 1 (C<sub>28</sub>H<sub>26</sub>KLaO<sub>23</sub>S<sub>4</sub>), calcd (%): C, 32.44; H, 2.53. Found: C, 32.69; H, 2.48. Elemental analysis for 2 (C<sub>28</sub>H<sub>26</sub>KNdO<sub>23</sub>S<sub>4</sub>), calcd (%): C, 32.27; H, 2.51. Found: C, 32.41; H, 2.55.

[LnK(AQDS)<sub>2</sub>(H<sub>2</sub>O)<sub>8</sub>]<sub>n</sub> (Ln = Gd (3) and Er (4)). The synthesis is similar as that for 1 and 2 except that Gd(NO<sub>3</sub>)<sub>3</sub>·6H<sub>2</sub>O (14.9 mg, 0.033 mmol) or ErCl<sub>3</sub>·6H<sub>2</sub>O (12.6 mg, 0.033 mmol) was used as the respective lanthanide salt. Plate-shaped red-brown-colored crystals appropriate for single-crystal X-ray diffractions were obtained. The crystals were separated by filtration, washed with methanol, and dried under vacuum. Yield: 72% for 3 and 78% for 4. Elemental analysis for 3 (C<sub>28</sub>H<sub>28</sub>ErK<sub>2</sub>O<sub>24</sub>S<sub>4</sub>), calcd (%): C, 31.05; H, 2.61. Found: C, 30.94; H, 2.51. Elemental analysis for 4 (C<sub>28</sub>H<sub>28</sub>GdK<sub>2</sub>O<sub>24</sub>S<sub>4</sub>), calcd (%): C, 31.34; H, 2.63. Found: C, 31.28; H, 2.59.

### 2.2. Typical procedure for oxidation of thioether

A mixture of catalyst (0.02 mmol) and thioether (0.4 mmol) in 2.0 mL methanol was added to a 25 mL Schlenk tube equipped with a magnetic stir bar. After the addition of 30% hydrogen peroxide (1.2 mmol), the reaction mixture was stirred at room temperature for 24 h in ambient air. Filtration was done after the reaction, and the filtrate was extracted with water/ethyl acetate for three times. The combined organic phase was dried over anhydrous Na<sub>2</sub>SO<sub>4</sub>, evaporated to dryness, and then subjected to column chromatography (silica gel, ethyl acetate) to afford pure sulfoxide product. The yields reported are based on the isolated pure product and characterization was performed by <sup>1</sup>H and <sup>13</sup>C NMR spectroscopy.

### 2.3. Single crystal X-ray crystallography

Single crystal X-ray diffraction data of all complexes were collected at 293 K on a Bruker APEX II CCD diffractometer operating at 50 KV and 30 mA using Mo K $\alpha$  radiation ( $\lambda = 0.71073 \text{ \AA}$ ). Data were integrated by SAINT and scaled with either a numerical or multi-scan absorption correction using SADABS. All structures were solved by direct methods or Patterson maps and refined by full-matrix least squares on *F*<sup>2</sup> using

SHELXL-2014 and OLEX2 program. All non-hydrogen atoms were refined anisotropically. Non-water hydrogen atoms were added at calculated positions and refined using a riding model. Hydrogen atoms of water molecules were located by different Fourier map and refined using riding model at restrained distance of 0.86 Å. Crystallographic data for all complexes are summarized in Table 1.

## 3. Results and discussion

With corresponding lanthanide salts and dipotassium anthraquinone-1,8-disulfonate, four bimetallic coordination complexes were synthesized using similar hydrothermal method, which include {[LnK(AQDS)<sub>2</sub>(H<sub>2</sub>O)<sub>4</sub>]·3H<sub>2</sub>O}<sub>n</sub> (Ln = La (1) or Nd (2)) and {[LnK(AQDS)<sub>2</sub>(H<sub>2</sub>O)<sub>8</sub>]<sub>n</sub> (Ln = Gd (3) or Er (4)). The isostructural complexes 1 and 2 crystallize in the monoclinic space group *P2*<sub>1</sub>/*n*. Each asymmetric unit comprises one Ln<sup>3+</sup> cation, one K<sup>+</sup> cation, two AQDS<sup>2-</sup> anions, four coordinated water molecules and three lattice water molecules (Fig. 1a). Detailed structural features will be discussed with complex 1 as an example hereafter. The nine-coordinated K<sup>+</sup> cation is surrounded by four AQDS<sup>2-</sup> anions, binding with sulfonate O atoms and carbonyl groups at distances between 2.656(6) to 3.266(5) Å. A couple of adjacent symmetry related K<sup>+</sup> cations are chelated by two symmetry related AQDS<sup>2-</sup> anions to form dimeric moiety with K...K separation of 4.095(6) Å. These dimeric moieties are further bridged by sulfonate O atoms of other symmetry related AQDS<sup>2-</sup> anions to constitute a column (Fig. 1b). It is interesting that  $\pi$ - $\pi$  stacking interactions also exist within the column and the centroid-to-centroid distances are 3.808(7) and 3.835(6) Å, which contribute to stabilizing the crystal packing (Fig. 1b). The coordination sphere of the K<sup>+</sup> cation is also complemented by a carbonyl O atom from another AQDS<sup>2-</sup> anion that chelates to the La<sup>3+</sup> cation. The La<sup>3+</sup> cation is also nine-coordinated. It is chelated on one end by an AQDS<sup>2-</sup> anion through two sulfonate groups and the carbonyl group in-between the sulfonate groups. On the other end, the La<sup>3+</sup> cation is chelated by two sulfonate groups of the dimeric [K-AQDS] moiety. The coordination sphere of the La<sup>3+</sup> cation is further complemented by four aqua ligands. The La – O bond distances range from 2.508(5) to 2.683(5) Å.

The two AQDS<sup>2-</sup> anions in the asymmetric unit take different coordination modes. One of them chelates the La<sup>3+</sup> cation through two sulfonate groups and the carbonyl group in-between the sulfonate groups, and the carbonyl group in the opposite side of the La<sup>3+</sup> cation bridges to the K<sup>+</sup> cation. The other AQDS<sup>2-</sup> ligand chelates to a couple of K<sup>+</sup> cations with two sulfonate groups and the carbonyl group in-between the sulfonate groups but the other carbonyl group has only hydrogen bonding interactions instead of coordination. The chelation with metal ions in both AQDS<sup>2-</sup> ligands leads to significant bending of the ligand, resulted in that the carbonyl group in-between the sulfonate groups falls out of the conjugation plane obviously. The dihedral angle between the C—C(=O)—C plane and the C<sub>14</sub> plane is 27.3(5)/9.3(5) for the AQDS<sup>2-</sup> ligand chelating to K<sup>+</sup> cation and 13.7(5)/7.7(5) for the other one binding with La<sup>3+</sup> cation.

Isostructural complexes 3 and 4 crystallize in the monoclinic space group *C2/c* and 4 will be used as an example for detailed structure description. The asymmetric unit contains one Er<sup>3+</sup> cation and one K<sup>+</sup> cation, two AQDS<sup>2-</sup> ligands, eight aqua ligands (Fig. 1c). The twelve-coordinated K<sup>+</sup> ion is chelated by two symmetry related AQDS<sup>2-</sup> ligands and two aqua ligands to form a subunit. These K<sup>+</sup> subunits were bridged by [Er(H<sub>2</sub>O)<sub>6</sub>]<sup>3+</sup> subunits through Er-sulfonate coordination, generating 1-D chain structure. The 1-D chains are further linked together by rich O—H...O hydrogen bonding to afford a 2-D layered structures, which further assemble into 3-D structure via  $\pi$ - $\pi$  stacking interactions. The Er-O bond lengths range from 2.307(2) to 2.366(2) Å and the K—O bond distances fall in the range of 2.766(2)–3.324(3) Å. The centroid-to-centroid distances of the  $\pi$ - $\pi$  stacking interactions are 3.634(2) and 3.822(19) Å (Fig. 1d). Similar as that in 1, the AQDS<sup>2-</sup> ligand also bends significantly to facilitate its chelation with metal ions,

**Table 1**  
Crystallographic data of complexes 1–4.

	1	2	3	4
Empirical formula	C <sub>28</sub> H <sub>26</sub> KO <sub>23</sub> S <sub>4</sub> La	C <sub>28</sub> H <sub>26</sub> KNdO <sub>23</sub> S <sub>4</sub>	C <sub>28</sub> H <sub>28</sub> KO <sub>24</sub> S <sub>4</sub> Gd	C <sub>28</sub> H <sub>28</sub> KO <sub>24</sub> S <sub>4</sub> Er
Fw	1036.74	1042.07	1073.09	1083.10
Crystal system	monoclinic	monoclinic	monoclinic	monoclinic
Space group	<i>P</i> 2 <sub>1</sub> / <i>n</i>	<i>P</i> 2 <sub>1</sub> / <i>n</i>	<i>C</i> 2/ <i>c</i>	<i>C</i> 2/ <i>c</i>
<i>a</i> (Å)	7.435(13)	7.398(3)	7.7884(13)	7.7514(5)
<i>b</i> (Å)	25.58(4)	25.308(8)	23.650(4)	23.8445(16)
<i>c</i> (Å)	19.02(3)	18.862(7)	19.883(3)	19.6001(13)
$\alpha$ (°)	90	90	90	90
$\beta$ (°)	95.39(4)	95.449(5)	95.685(2)	96.383(2)
$\gamma$ (°)	90	90	90	90
<i>V</i> (Å <sup>3</sup> )	3602(10)	3516(2)	3644.4(10)	3600.2(4)
<i>Z</i>	4	4	4	4
$\rho_{\text{cal}}$ (g·cm <sup>-3</sup> )	1.912	1.969	1.956	1.998
$\mu$ (mm <sup>-1</sup> )	1.628	1.930	2.261	2.777
<i>F</i> (000)	2072.0	2084.0	2140	2156
Goodness-of-fit on <i>F</i> <sup>2</sup>	1.020	1.009	1.052	1.063
<i>R</i> <sub>1</sub> <sup>a</sup> , <i>wR</i> <sub>2</sub> <sup>b</sup> [ <i>I</i> > 2 $\sigma$ ( <i>I</i> )]	0.0448, 0.0708	0.0554, 0.0862	0.0304, 0.0706	0.0260, 0.0619
<i>R</i> <sub>1</sub> <sup>a</sup> , <i>wR</i> <sub>2</sub> <sup>b</sup> (all data)	0.0912, 0.0833	0.1173, 0.1052	0.0356, 0.0736	0.0308, 0.0635
( $\Delta\rho$ ) <sub>max</sub> / <sub>min</sub> (e Å <sup>-3</sup> )	0.69/-0.75	1.44/-0.98	0.947/-0.616	0.521/-0.532

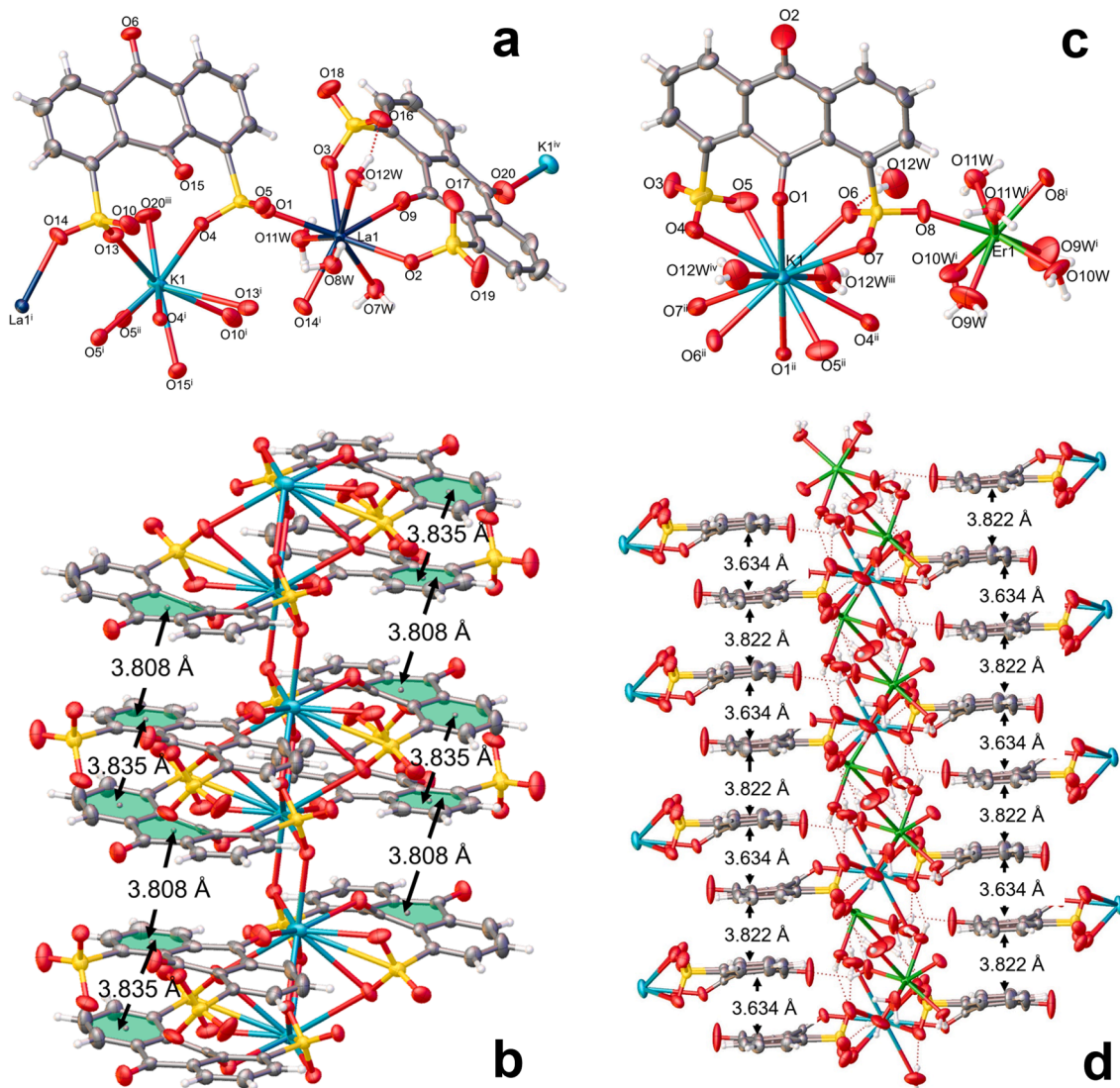


**Fig. 1.** (a) The asymmetric unit in 1 showing coordination geometries of metal centers and binding modes of the ligands. Symmetry codes: <sup>i</sup>2-*X*,1-*Y*,1-*Z*; <sup>ii</sup>1 + *X*,+*Y*,+*Z*; <sup>iii</sup>1/2 + *X*,3/2-*Y*,-1/2 + *Z*; <sup>iv</sup>-1/2 + *X*,3/2-*Y*,1/2 + *Z*. Lattice water omitted for clarity. (b) The  $\pi$  -  $\pi$  stacking interactions in complex 1. (c) The asymmetric unit in 4 showing coordination geometries of metal centers and binding mode of the ligand. Symmetry codes: <sup>i</sup>-*X*,+*Y*,3/2-*Z*; <sup>ii</sup>1-*X*,1-*Y*,1-*Z*; <sup>iii</sup>-*X*,1-*Y*,1-*Z*; <sup>iv</sup>1 + *X*,+*Y*,+*Z*. (d) The  $\pi$  -  $\pi$  stacking interactions in complex 4.

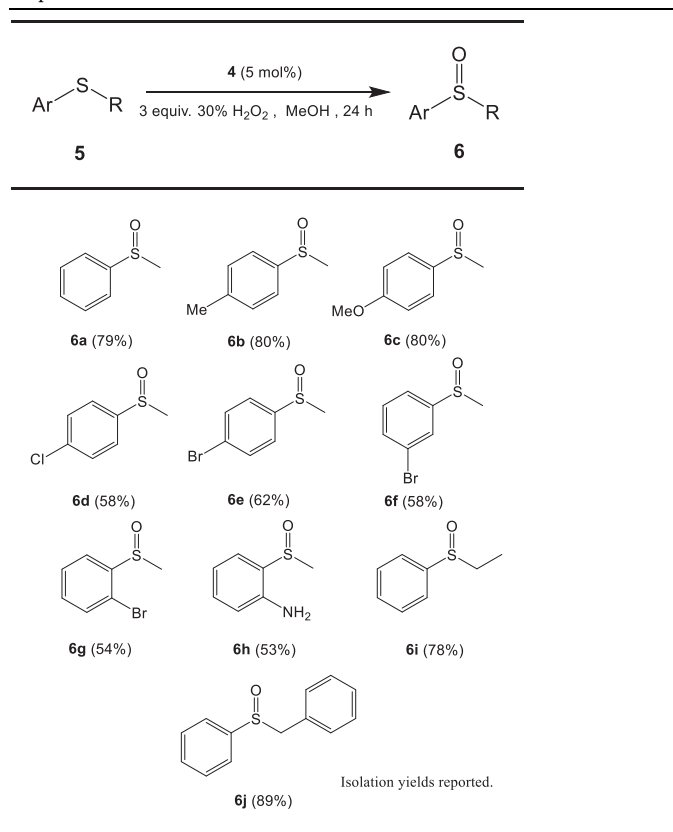
and the dihedral angle between the C—C(=O)—C plane and the C<sub>14</sub> plane is 24.6(2)/15.0(3), indicating more bending of the ligand compared to that in 1.

Quinones have been used as catalysts in oxidation reactions, and therefore these lanthanide complexes were subjected to the investigation of catalytic studies for oxidation of thioethers. With methyl phenyl sulfide as the reaction substrate, the optimized reaction conditions were studied systematically over a variety of factors including catalysts, solvents and oxidants (Table S3). Control experiment without catalyst showed that hydrogen peroxide itself can oxidize thioether at limited yield (Entry 1). K<sub>2</sub>AQDS catalyzes the oxidation in moderate yield while no reaction occurs without oxidant (Entry 2 and 3). Only trace amount of product was observed with O<sub>2</sub> as the oxidant (Entry 4). Methanol is the only one among the commonly used solvents which produces satisfactory yield (Entries 5–10). Similar yields were obtained with 5% or 10% catalyst (Entry 5 and 11). The optimal reaction conditions thus obtained was the use of methanol as solvent and hydrogen peroxide as oxidant with 5% catalyst. Screening of the catalyst with the optimal reaction condition indicated that complex 4 has the best catalytic efficiency (Table S4).

The catalysts have some solubility in methanol, although not good enough to be fully soluble in the amount of solvent used for the reaction, under which conditions the recovery rate of the catalyst was about 60%. Therefore no cycle experiments were performed. The catalytic process was believed to be homogenous, which means the amount of catalyst that dissolved into the solvent actually catalyzed the reaction. This explains why the use of 5% and 10% molar ratio catalyst would lead to almost the same yield (entry 5 and 11 in Table S3), because what takes effect was those dissolved into the reaction medium (the amount of solvent were the same for both reactions).

Under the optimal reaction conditions, various thioether substrates were investigated to study the versatility and substrate scope of this

**Table 2**  
Scope of thioethers.



catalytic system (Table 2). The results showed that electron-donating substituents on the phenyl ring of aryl methyl sulfides facilitate the oxidation reaction and result in high yield of 80% (6b, 6c), being comparable with that of methyl phenyl sulfide (6a). However, the yield for the oxidation product 6h was only 53%, although there was an electron-donating amino group on the *ortho*-position of the phenyl ring. Electron-withdrawing group on the phenyl ring (regardless of substitution position) (6d–6g) led to less efficient oxidation, the yields being at medium level of 54–62%. Para-bromo phenyl methyl sulfide could be oxidized at 62% yield (6e) and *meta*-bromo phenyl methyl sulfide was oxidized with 58% yield (6f), while oxidation of *ortho*-bromo phenyl methyl sulfide afforded only 54% product yield (6g). Oxidation of the ethyl phenyl sulfide (2i) gives similar yield as that for methyl phenyl sulfide (6a). The best oxidation yield was obtained with benzyl phenyl sulfide, which was the highest of 89% (6j).

A possible reaction mechanism has been proposed for this oxidation reaction (see Fig. 2) [43,44]. Our previous research over anthraquinone derivative ligands indicated that their coordination complexes are good catalysts for photooxidation reactions, based on the transformation among the cycle of catalyst (M-L), photoexcited form (M-L\*), and semi-hydroquinone radical form (M-L(H)<sup>•</sup>) [38]. However in this case, the complexes can catalyze the oxidation reaction without photoexcitation, which can be correlated with the unique structure feature of the complexes. As mentioned in the structural description, the ligands in all these complexes take chelation mode, which results in remarkable steric effect. One of the carbonyl groups bends out of the conjugated plane significantly, dictating the fact that the generation of semi-hydroquinone form would be much easier as compared to previous cases without obvious structural bending. And this explains why this series of complexes are able to catalyze the oxidation reaction without any need of photooxidation.

#### 4. Conclusions

In summary, four lanthanide-potassium bimetallic coordination complexes have been synthesized with anthraquinone-1,8-disulfonate as the dianionic ligand. Single-crystal X-ray structure analysis revealed that the complexes belong to two isostructural series, with rich hydrogen bonding and  $\pi$ - $\pi$  stacking interaction to stabilize the crystal packing. The ligands in 1 and 2 chelate with either lanthanide or K<sup>+</sup> ions while that in 3 and 4 chelate only with K<sup>+</sup> ions, in addition to their bridging roles in all cases. The chelation modes involving the coordination of carbonyl group exerted significant steric effect to push the carbonyl group out of the conjugation plane, resulting in easier hydrogenation to form the semi-hydroquinone intermediate, which endows the complexes with good catalytic properties toward oxidation of thioethers. Complex 4 among the series demonstrated the best catalytic efficiency over a wide range of substrates.

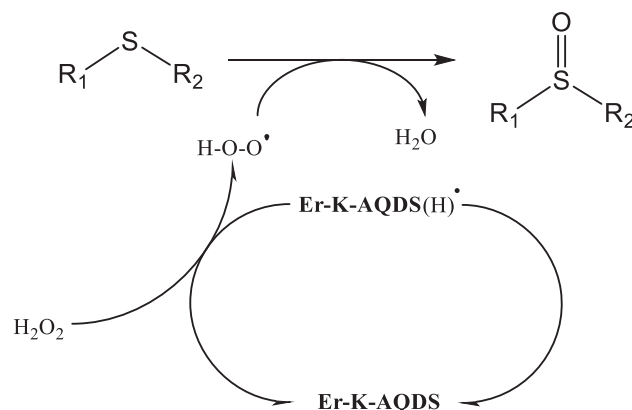


**Fig. 2.** Proposed reaction mechanism of the oxidation reaction.

## CRedit authorship contribution statement

**Fu-Yu Cao:** Investigation, Formal analysis, Methodology, Writing - original draft. **Meng-Ping Huang:** Investigation. **Hui-Lei Gao:** Investigation. **Xiao-Li Zhao:** Writing - review & editing. **Jie Han:** Writing - review & editing. **Xu-Dong Chen:** Conceptualization, Supervision, Writing - review & editing, Funding acquisition.

## Declaration of Competing Interest

The authors declare that they have no known competing financial interests or personal relationships that could have appeared to influence the work reported in this paper.

## Acknowledgments

This work was supported by the National Natural Science Foundation of China (21671104, 22071110), the Priority Academic Program Development of Jiangsu Higher Educational Institutions, the Jiangsu Collaborative Innovation Center of Biomedical Functional Materials.

## Appendix A. Supplementary material

X-ray crystallographic data for complexes **1-4** have been deposited with the Cambridge Crystallographic Data Center (CCDC Numbers 2059803 for complex **1**; 2070118-2070120 for complex **2-4**).

Supplementary data to this article can be found online at <https://doi.org/10.1016/j.inoche.2021.108682>.

## References

- B. Li, H.M. Wen, Y. Cui, G.D. Qian, B.L. Chen, Multifunctional lanthanide coordination polymers, *Prog. Polym. Sci.* 48 (2015) 40–84.
- T. Devic, C. Serre, N. Audebrand, J. Marrot, G. Férey, MIL-103, A 3-D lanthanide-based metal organic framework with large one-dimensional tunnels and a high surface area, *J. Am. Chem. Soc.* 127 (2005) 12788–12789.
- L.J. Zhou, W.H. Deng, Y.L. Wang, G. Xu, S.G. Yin, Q.Y. Liu, Lanthanide-potassium biphenyl-3,3'-disulfonyl-4,4'-dicarboxylate frameworks: gas sorption, proton conductivity, and luminescent sensing of metal ions, *Inorg. Chem.* 55 (2016) 6271–6277.
- R. Liu, Q.Y. Liu, R. Krishna, W.J. Wang, C.T. He, Y.L. Wang, Water-stable Europium 1,3,6,8-tetrakis(4-carboxylphenyl)pyrene framework for efficient C<sub>2</sub>H<sub>2</sub>/CO<sub>2</sub> separation, *Inorg. Chem.* 58 (2019) 5089–5095.
- W.R. Lee, D.W. Ryu, J.W. Lee, J.H. Yoon, E.K. Koh, C.S. Hong, Microporous lanthanide-organic frameworks with open metal sites: unexpected sorption propensity and multifunctional properties, *Inorg. Chem.* 49 (2010) 4723–4725.
- Q.Y. Yang, M. Pan, S.C. Wei, K. Li, B.B. Du, C.Y. Su, Linear dependence of photoluminescence in mixed Ln-MOFs for color tunability and barcode application, *Inorg. Chem.* 54 (2015) 5707–5716.
- Y.N. Wang, S.D. Wang, W.J. Wang, X.X. Hao, H. Qi, Ln-CPs constructed from unsymmetrical tetracarboxylic acid ligand: tunable white-light emission and highly sensitive detection of CrO<sub>4</sub><sup>2-</sup>, Cr<sub>2</sub>O<sub>7</sub><sup>2-</sup>, MnO<sub>4</sub><sup>-</sup> in water, *Spectrochim. Acta A* 229 (2020), 117915.
- D. Zhao, X.T. Rao, J.C. Yu, Y.J. Cui, Y. Yang, G.D. Qian, Syntheses, structures and tunable luminescence of lanthanide metal-organic frameworks based on azole-containing carboxylic acid ligand, *J. Solid State Chem.* 230 (2015) 287–292.
- Q. Tang, S.X. Liu, Y.W. Liu, D.F. He, J. Miao, X.Q. Wang, Y.J. Ji, Z.P. Zheng, Color tuning and white light emission via in situ doping of luminescent lanthanide metal-organic frameworks, *Inorg. Chem.* 53 (2014) 289–293.
- M.L. Gao, W.J. Wang, L. Liu, Z.B. Han, N. Wei, X.M. Cao, D.Q. Yuan, Microporous hexanuclear Ln(III) cluster-based metal-organic frameworks: color tunability for barcode application and selective removal of methylene blue, *Inorg. Chem.* 56 (2017) 511–517.
- L. Liu, X.N. Zhang, Z.B. Han, M.L. Gao, X.M. Cao, S.M. Wang, An Ln<sup>III</sup>-based anionic metal-organic framework: sensitization of lanthanide (III) ions and selective absorption and separation of cationic dyes, *J. Mater. Chem. A* 3 (2015) 14157–14164.
- W.W. Zhang, Y.L. Wang, Q.Y. Liu, Q.Y. Liu, Lanthanide-benzophenone-3,3'-disulfonyl-4,4'-dicarboxylate frameworks: temperature and 1-hydroxypyrene luminescence sensing and proton conduction, *Inorg. Chem.* 57 (2018) 7805–7814.
- P. Mahata, S.K. Mondal, D.K. Singha, P. Majee, Luminescent rare-earth-based MOFs as optical sensors, *Dalton Trans.* 46 (2017) 301–328.
- B. Yan, Lanthanide-functionalized metal-organic framework hybrid systems to create multiple luminescent centers for chemical sensing, *Acc. Chem. Res.* 50 (2017) 2789–2798.
- J. Zhou, T.T. Zhu, J. Han, X.D. Chen, Lanthanide(III)-organic extended frameworks based on cubic [Ln<sub>4</sub>(μ<sub>3</sub>-OH)<sub>4</sub>] clusters: syntheses, structures and application as fluorescent sensor, *Inorg. Chem. Commun.* 108 (2019), 107536.
- J. Rocha, C.D.S. Brites, L.D. Carlos, Lanthanide organic framework luminescent thermometers, *Chem. Eur. J.* 22 (2016) 14782–14795.
- X.T. Rao, T. Song, J.K. Gao, Y.J. Cui, Y. Yang, C.D. Wu, B.L. Chen, G.D. Qian, A highly sensitive mixed lanthanide metal-organic framework self-calibrated luminescent thermometer, *J. Am. Chem. Soc.* 135 (2013) 15559–15564.
- B.V. Harbuzaru, A. Corma, F. Rey, J.L. Jorda, D. Ananias, L.D. Carlos, J. Rocha, A miniaturized linear pH sensor based on a highly photoluminescent self-assembled Europium(III) metal-organic framework, *Angew. Chem. Int. Ed.* 48 (2009) 6476–6479.
- Y.W. Ren, J.X. Liang, J.X. Lu, B.W. Cai, D.B. Shi, C.R. Qi, H.F. Jiang, J. Chen, D. Zheng, 1,4-phenylenediacetate-based Ln MOFs - synthesis, structures, luminescence, and catalytic activity, *Eur. J. Inorg. Chem.* 2011 (2011) 4369–4376.
- M. Gustafsson, A. Bartoszewicz, B. Martín-Matute, J.L. Sun, J. Grins, T. Zhao, Z. Y. Li, G.S. Zhu, X.D. Zou, A family of highly stable lanthanide metal-organic frameworks: structural evolution and catalytic activity, *Chem. Mater.* 22 (2010) 3316–3322.
- P.Y. Wu, J. Wang, Y.M. Li, C. He, Z. Xie, C.Y. Duan, Luminescent sensing and catalytic performances of a multifunctional lanthanide-organic framework comprising a triphenylamine moiety, *Adv. Funct. Mater.* 21 (2011) 2788–2794.
- L. Cunha-Silva, S. Lima, D. Ananias, P. Silva, L. Mafra, L.D. Carlos, M. Pillinger, A. A. Valente, F.A. Almeida Paz, J. Rocha, Multi-functional rare-earth hybrid layered networks: photoluminescence and catalysis studies, *J. Mater. Chem.* 19 (2009) 2618–2632.
- J.W. Han, C.L. Hill, A coordination network that catalyzes O<sub>2</sub>-based oxidations, *J. Am. Chem. Soc.* 129 (2007) 15094–15095.
- F. Gándara, E.G. Puebla, M. Iglesias, D.M. Proserpio, N. Snejko, M.Á. Monge, Controlling the structure of arenedisulfonates toward catalytically active materials, *Chem. Mater.* 21 (2009) 655–661.
- N. Wei, M.Y. Zhang, X.N. Zhang, G.M. Li, X.D. Zhang, Z.B. Han, Two series of solvent-dependent lanthanide coordination polymers demonstrating tunable luminescence and catalysis properties, *Cryst. Growth Des.* 14 (2014) 3002–3009.
- H.H. Wang, L.J. Zhou, Y.L. Wang, Q.Y. Liu, Terbium-biphenyl-3,3'-disulfonyl-4,4'-dicarboxylate framework with sulfonate sites for luminescent sensing of Cr<sup>3+</sup> ion, *Inorg. Chem. Commun.* 73 (2016) 94–97.
- G.K.H. Shimizu, R. Vaidhyanathan, J.M. Taylor, Phosphonate and sulfonate metal organic frameworks, *Chem. Soc. Rev.* 38 (2009) 1430–1449.
- G.Y. Zhang, H.H. Fei, Synthesis and applications of porous organosulfonate-based metal-organic frameworks, *Top. Curr. Chem.* 377 (2019) 32.
- G.Y. Zhang, G.F. Wei, Z.P. Liu, S.R.J. Oliver, H.H. Fei, A robust sulfonate-based metal-organic framework with permanent porosity for efficient CO<sub>2</sub> capture and conversion, *Chem. Mater.* 28 (2016) 6276–6281.
- A.V. Desai, B. Joarder, A. Roy, P. Samanta, R. Babarao, S.K. Ghosh, Multifunctional behavior of sulfonate-based hydrolytically stable microporous metal-organic frameworks, *ACS Appl. Mater. Interfaces* 10 (2018) 39049–39055.
- W.J. Liu, N. Wang, Z.Q. Wei, X. Zhao, L.M. Chang, S.T. Yue, Y.L. Liu, Y.P. Cai, Controllable assembly of organodisulfonate complexes with tuned mole ratios: From 0D to 3D networks, *Inorg. Chem. Commun.* 14 (2011) 1807–1814.
- A. Kawamura, A.S. Filatov, J.S. Anderson, Sulfonate-ligated coordination polymers incorporating paramagnetic transition metals, *Eur. J. Inorg. Chem.* 2019 (2019) 2613–2617.
- E.E. Langdon-Jones, S.J.A. Pope, The coordination chemistry of substituted anthraquinones: Developments and applications, *Coordin. Chem. Rev.* 269 (2014) 32–53.
- L.B. Zhao, S.T. Gao, R.X. He, W. Shen, M. Li, Molecular design of phenanthrenequinone derivatives as organic cathode materials, *ChemSusChem* 11 (2018) 1215–1222.
- Z.Y. Zhang, H. Yoshikawa, K. Awaga, Monitoring the solid-state electrochemistry of Cu(2,7-AQDC) (AQDC = anthraquinone dicarboxylate) in a lithium battery: coexistence of metal and ligand redox activities in a metal-organic framework, *J. Am. Chem. Soc.* 136 (2014) 16112–16115.
- P.J. Celis-Salazar, C.C. Epley, S.R. Ahrenholtz, W.A. Maza, P.M. Usov, A.J. Morris, Proton-coupled electron transport in anthraquinone-based zirconium metal-organic frameworks, *Inorg. Chem.* 56 (2017) 13741–13747.
- A.E. Platero-Prats, M. Iglesias, N. Snejko, A. Monge, E. Gutiérrez-Puebla, From coordinatively weak ability of constituents to very stable alkaline-earth sulfonate metal-organic frameworks, *Cryst. Growth Des.* 11 (2011) 1750–1758.
- C.P. Ye, G. Xu, Z. Wang, J. Han, L. Xue, F.Y. Cao, Q. Zhang, L.F. Yang, L.Z. Lin, X. D. Chen, Design and synthesis of functionalized coordination polymers as recyclable heterogeneous photocatalysts, *Dalton Trans.* 47 (2018) 6470–6478.
- C.P. Ye, R. Ling, L.F. Yang, Q. Zhang, J. Han, X.D. Chen, Syntheses, crystal structures and photocatalytic properties of transition metal complexes based on 9,10-anthraquinone-1,3-dicarboxylate, *Transit. Metal Chem.* 44 (2019) 475–482.
- R.F. D'Vries, N. Snejko, E. Gutiérrez-Puebla, M. Iglesias, M. Angeles Monge, Supramolecular structures via hydrogen bonds and π-stacking interactions in novel anthraquinonedisulfonates of zinc, nickel, cobalt, copper and manganese, *Inorg. Chim. Acta* 382 (2012) 119–126.
- X.X. Yang, W.D. Yu, X.Y. Yi, C. Liu, Accurate regulating of visible-light absorption in polyoxotitanate-calix[8]arene systems by ligand modification, *Inorg. Chem.* 59 (2020) 7512–7519.
- I. Reviejo, V. Taberner, M.E.G. Mosquera, J. Ramos, T. Cuenca, G. Jiménez, Chiral Titanium(IV) complexes containing polydentate ligands based on α-pi-nene.

- catalytic activity in sulfoxidation with hydrogen peroxide, *Organometallics* 37 (2018) 3437–3449.
- [43] Y. Zhang, W.D. Yu, B. Li, Z.F. Chen, J. Yan, Discovery of a new family of polyoxometalate-based hybrids with improved catalytic performances for selective sulfoxidation: the synergy between classic heptamolybdate anions and complex cations, *Inorg. Chem.* 58 (2019) 14876–14884.
- [44] R. Hasanpour, F. Feizpour, M. Jafarpour, A. Rezaeifard, Nickel(II) riboflavin complex as an efficient nanobiocatalyst for heterogeneous and sustainable oxidation of benzylic alcohols and sulfides, *New J. Chem.* 42 (2018) 7383–7391.